Arch. Mech., 49, 4, pp. 791–804, Warszawa 1997

Dynamic response of a fluid-saturated elastic porous solid

S. BREUER (ESSEN)

IN THIS PAPER, the field equations governing the dynamic response of a fluid-saturated elastic porous media are analyzed and built up for the study of the consolidation problem and the one-dimensional wave propagation. The two constituents are assumed to be incompressible. A one-dimensional numerical solution is derived by means of the standard Galerkin procedure and the finite element method. As a result of the incompressibility, there is only one independent dilatational wave propagating in the solid and the fluid phase. This work can provide further understanding of the wave propagation in porous materials, not only in view of the propagation speed, but also with respect to the development of the amplitudes.

1. Introduction

A FLUID-SATURATED POROUS MEDIUM is a portion of space occupied partly by a solid phase (solid skeleton) and partly by a void space filled with fluid, e.g. water. The mechanical behaviour of such a medium is governed mainly by the interaction of the solid skeleton with the fluid. This interaction occurs in quasi-static problems, like foundations, but is particularly strong in dynamic problems, for example earthquakes. In contrast to wave propagation in one-component bodies, the wave propagation in a porous medium has special characteristics. As usual, we have two different kinds of waves, the compression (longitudinal) wave and the shear (transversal) wave. But in a porous medium with compressible constituents, the compression wave has two different velocities, a fast P1 wave and a slow P2 wave. In this contribution, however, the constituents are assumed to be incompressible and as a result of this assumption, the P1 velocity is infinite.

The two-phase behaviour of a fluid-saturated porous medium can only be predicted quantitatively by elaborate numerical computation, which fortunately is possible today due to the development of powerful computers.

Many computations done in the field of dynamics of porous media have made use of BIOT'S theory [1], because Biot's theory leads to quite good results for linear elastic problems. But as this theory has not been developed from the basic equations of mechanics, its further development causes many problems.

In this investigation, the calculation of the dynamic response of a fluid-saturated elastic porous solid is based upon the macroscopic porous media theory

(TPM – Theory of Porous Media), which is defined as the mixture theory restricted by the volume fraction concept. Readers interested in details of this theory are referred to the papers of de BOER [8], BLUHM [2], BLUHM and DE BOER [3], EHLERS [10] and BOWEN [4, 5]. In order to simplify the problem, thermal effects and exchanges of mass between the constituents are excluded, and single constituents are treated as incompressible.

In Sec. 2 the governing equations of the above mentioned theory are discussed and the field equations and constitutive relations are taken into account. In the third section these equations are built up for the numerical computation. The finite element method is used for the discretisation of the basic equations and the time integration is done by the Newmark method. In Sec. 4 the dynamic consolidation problem of a one-dimensional elastic porous body and the wave propagation in this medium is investigated. Solutions obtained by the finite element method are compared with the existing analytical solutions based on the same theory. This paper ends with some concluding remarks in Sec. 5.

2. Governing equations

2.1. Kinematics and the concept of volume fraction

Considering the kinematics of the fluid-saturated porous medium, which is an immiscible mixture of the constituents φ^α with particles X^α ($\alpha = S$: solid phase, $\alpha = F$: fluid phase), it is assumed that at any time t each spatial point is simultaneously occupied by the particles X^S and X^F. These particles X^α proceed from different reference positions $\mathbf{X}_\alpha$ at time $t = t_0$. Thus, each constituent is assigned its own independent motion function $\boldsymbol{\chi}_\alpha$, from which the velocity $\mathbf{x}'_\alpha$, the acceleration $\mathbf{x}''_\alpha$ and the deformation gradient $\mathbf{F}_\alpha$ can be calculated:

$$\mathbf{x} = \boldsymbol{\chi}_\alpha(\mathbf{X}_\alpha, t), \qquad \mathbf{x}'_\alpha = \mathbf{x}'_\alpha(\mathbf{X}_\alpha, t), \qquad \mathbf{x}''_\alpha = \mathbf{x}''_\alpha(\mathbf{X}_\alpha, t), \qquad \mathbf{F}_\alpha = \operatorname{Grad}_\alpha \boldsymbol{\chi}_\alpha,$$

where $\operatorname{Grad}_\alpha$ means the derivative with respect to $\mathbf{X}_\alpha$. The volume fractions

$$n^\alpha = n^\alpha(\mathbf{x}, t)$$

are defined as the local ratios of the constituent volumes v^α with respect to the bulk volume v of the control space B_S, which is shaped by the solid skeleton

$$dv^\alpha = n^\alpha \, dv, \qquad v^\alpha = \int_{B_S} n^\alpha \, dv.$$

With the aid of the volume fractions

$$v = \int_{B_S} dv = \sum_{\alpha=1}^{\kappa} v^\alpha = \int_{B_S} \sum_{\alpha=1}^{\kappa} dv^\alpha = \int_{B_S} \sum_{\alpha=1}^{\kappa} n^\alpha \, dv,$$

we get the volume fraction condition

$$\sum_{\alpha=1}^{\kappa} n^\alpha = 1. \tag{2.1}$$

The volume fraction condition (2.1) plays an important role as a constraint in the constitutive theory of porous media, see DE BOER [8] or BLUHM and DE BOER [3].

Each of the constituents φ^α has a real density $\varrho^{\alpha R}$, which is defined as the mass of φ^α per unit of v^α. With the aid of the volume fraction concept, these properties can be "smeared" over the control space and we obtain the partial density

$$\varrho^\alpha = n^\alpha \varrho^{\alpha R}.$$

2.2. Field equations

Excluding mass exchanges and thermal effects, the mechanical behavior of a fluid-saturated porous solid is described in BLUHM [2] and EHLERS [10] by the balance equation of mass for each single constituent

$$(\varrho^\alpha)'_\alpha + \varrho^\alpha \operatorname{div} \mathbf{x}'_\alpha = 0, \tag{2.2}$$

the balance equation of momentum

$$\operatorname{div} \mathbf{T}^\alpha + \varrho^\alpha(\mathbf{b} - \mathbf{x}''_\alpha) + \mathbf{s}^\alpha = \mathbf{0}, \tag{2.3}$$

and the volume fraction condition that changes for a binary mixture into the saturation condition

$$n^S + n^F = 1. \tag{2.4}$$

In these equations $\mathbf{T}^\alpha$ is the partial Cauchy stress tensor, $\mathbf{b}$ the external acceleration, and $\mathbf{s}^\alpha$ the interaction force of the constituents. In addition, "div" is the divergence operator and the symbol $(\ldots)'_\alpha$ denotes the material time derivative with respect to the trajectory of φ^α.

As the sum of the interaction forces must vanish, we obtain for a binary mixture

$$\mathbf{s}^F + \mathbf{s}^S = \mathbf{0}.$$

The balance equation of moment of momentum leads, excluding any moment of momentum supply, to a symmetric stress tensor

$$\mathbf{T}^\alpha = \mathbf{T}^{\alpha T}.$$

2.3. Constitutive relations

Since the number of unknown fields $(\mathbf{T}^\alpha, \boldsymbol{\chi}^\alpha, \mathbf{s}^\alpha)$ is larger than the number of field equations, we have to introduce constitutive relations for $\mathbf{T}^\alpha$, $\mathbf{s}^\alpha$ and the density $\varrho^{\alpha R}$. As both constituents are incompressible, we have

$$\varrho^{\alpha R} = \text{constant}.$$

With this assumption, the volume fractions can be calculated from the balance equations of mass (2.2) and with the aid of the deformation gradient, one obtains

$$n^\alpha = n^{\alpha 0} \, (\det \mathbf{F}_\alpha)^{-1},$$

where $n^{\alpha 0}$ describes the initial porosity of φ^α.

The constitutive relations for the solid and fluid stress tensor $\mathbf{T}^\alpha$ and for the interaction force $\mathbf{s}^\alpha$ $(\alpha = S, F)$ consist of two terms, where the former, as a result of the saturation condition, is proportional to the pore pressure p, while the latter represents the extra quantities, index $(...)_E$, determined by the deformation:

$$\begin{aligned} \mathbf{T}^\alpha &= -n^\alpha \, p \, \mathbf{I} + \mathbf{T}^\alpha_E \,, \\ \mathbf{s}^F &= p \, \mathrm{grad} \, n^F + \mathbf{s}^F_E \,. \end{aligned}$$

The partial effective stress tensor of the fluid can be neglected:

$$\mathbf{T}^F_E \approx \mathbf{0},$$

and the partial effective stress tensor of the solid can be expressed by the law of SIMO and PISTER [12]:

$$\mathbf{T}^S_E = \frac{1}{\det \mathbf{F}_S} \left(\mu^S \mathbf{B}_S + \left[\lambda^S \ln(\det \mathbf{F}_S) - \mu^S \right] \mathbf{I} \right),$$

where λ^S and μ^S are the Lamé constants of the solid material and $\mathbf{B}_S = \mathbf{F}_S \, \mathbf{F}_S^T$ is the left Cauchy - Green tensor.

The interaction between the fluid and solid constituents, caused by the motions, can be described by the extra supply term of momentum

$$\mathbf{s}^F_E = -\frac{(n^F)^2 \, \gamma^{FR}}{k^F} \mathbf{w}_F \,,$$

with $\mathbf{w}_F = (\mathbf{x}'_F - \mathbf{x}'_S)$ being the seepage velocity, γ^{FR} the real specific weight of the fluid and k^F the Darcy permeability parameter.

3. Numerical solution concept

3.1. Solution strategy

An effective way to solve the system of equations and to match the problem to the boundary and initial conditions consists in combining the balance equations of momentum (2.3) of both constituents

$$\operatorname{div}(\mathbf{T}^S + \mathbf{T}^F) + (\varrho^S + \varrho^F)\mathbf{b} - \varrho^S \mathbf{x}''_S - \varrho^F \left[(\mathbf{w}_F + \mathbf{x}'_S)'_S + \operatorname{grad}(\mathbf{w}_F + \mathbf{x}'_S)\,\mathbf{w}_F\right] = \mathbf{0} \tag{3.1}$$

as well as the balance equation of momentum of the fluid,

$$\operatorname{div}\mathbf{T}^F + \varrho^F \left(\mathbf{b} - \left[(\mathbf{w}_F + \mathbf{x}'_S)'_S + \operatorname{grad}(\mathbf{w}_F + \mathbf{x}'_S)\mathbf{w}_F\right]\right) - \frac{\gamma^{FR}(n^F)^2}{k^f}\,\mathbf{w}_F = \mathbf{0}. \tag{3.2}$$

The remaining equations and unknowns can be substituted by a combination of the balance equations of mass (2.2) together with the saturation condition (2.4). Considering the incompressibility of both constituents, we get:

$$\operatorname{div}(n^F \mathbf{w}_F + \mathbf{x}'_S) = 0. \tag{3.3}$$

In these equations the fluid velocity $\mathbf{x}'_F$ is replaced by $\mathbf{x}'_F = \mathbf{w}_F + \mathbf{x}'_S$, for a better fit to the boundary conditions. For example, at an undrained boundary it causes less problems to prescribe $\mathbf{w}_F = 0$, i.e., $\mathbf{x}'_S = \mathbf{x}'_F$.

3.2. Weak formulation

For numerical computations, a standard Galerkin procedure was chosen. Therefore, each of the basic equations (3.1), (3.2), (3.3) has to be multiplied by a weighting function. For Eq. (3.1), a virtual solid displacement $\bar{\mathbf{u}}_S$ is chosen. The volume integral of a divergence can be transformed, see DE BOER [7], into a surface integral

$$\int_B \Big\{(\mathbf{T}^S_E - p\,\mathbf{I})\cdot\operatorname{grad}\bar{\mathbf{u}}_S + \varrho^S\,\mathbf{x}''_S\cdot\bar{\mathbf{u}}_S + \varrho^F\left[(\mathbf{w}_F + \mathbf{x}'_S)'_S + \operatorname{grad}(\mathbf{w}_F + \mathbf{x}'_S)\mathbf{w}_F\right]\cdot\bar{\mathbf{u}}_S\Big\}\,dv = \int_A \mathbf{t}\cdot\bar{\mathbf{u}}_S\,da + \int_B (\varrho^S + \varrho^F)\mathbf{b}\cdot\bar{\mathbf{u}}_S\,dv,$$

where $\mathbf{t}$ is the stress vector on the surface of the mixture, including the stress on the solid and the stress on the fluid.

For Eq. (3.2), a virtual seepage velocity $\bar{\mathbf{w}}_F$ was taken into account and the volume integral was transformed into a surface integral

$$\int_B \Big\{(-p \operatorname{div} \bar{\mathbf{w}}_F) + \frac{\gamma^{FR} n^F}{kf} \mathbf{w}_F \cdot \bar{\mathbf{w}}_F + \varrho^{FR}\Big[(\mathbf{w}_F + \mathbf{x}'_S)'_S$$

$$+ \operatorname{grad}(\mathbf{w}_F + \mathbf{x}'_S)\mathbf{w}_F\Big] \cdot \bar{\mathbf{w}}_F\Big\} dv = -\int_A p\, \bar{\mathbf{w}}_F \cdot \mathbf{n}\, da + \int_B \varrho^{FR}\, \mathbf{b} \cdot \bar{\mathbf{w}}_F\, dv.$$

Equation (3.3) represents the saturation condition together with the mass balance equations, and it has been multiplied by a virtual pressure $\bar{p}$

$$\int_B \operatorname{div}\left(n^F \mathbf{w}_F + \mathbf{x}'_S\right) \bar{p}\, dv = 0.$$

3.3. Solution algorithm

From the weak formulation, one gets 3 scalar equations with the unknown functions $(\mathbf{u}_S, \mathbf{w}_F, p)$. For the discretisation of the problem, the unknown functions $(\mathbf{u}_S, \mathbf{w}_F, p)$, as well as their time derivatives and the corresponding weighting functions $(\bar{\mathbf{u}}_S, \bar{\mathbf{w}}_F, \bar{p})$ are approximated by linear shape functions. Since the values of the weight functions are not specified, the coefficient multiplied by the value of the weight function must vanish. Now, the 3 scalar equations of the weak formulation are split into n equations, where n is the number of unknowns at each node, multiplied by the number of nodes per element. Thus, the discretisation of the problem leads to a system of n equations with the unknowns $(\mathbf{u}_S, \mathbf{u}'_S, \mathbf{u}''_S, \mathbf{w}_F, \mathbf{w}'_F, p)$. The matrix of the coefficients multiplied by the value of the discrete unknowns are denoted by **M**, **D**, **K**. **M** means the mass matrix and is connected with the second time derivative of the unknowns. **D** represents the damping matrix and is coupled with the first time derivative of the unknowns, and at last **K** denotes the stiffness matrix and is connected with the unknowns. The index M, F or K in Eq. (3.4) means, that these coefficients come from the balance equation of mixture (M), the balance equation of fluid (F) or from the saturation condition (K). The second index represents the kind of unknowns, 1 stands for the motion of solid, 2 for the motion of fluid and 3 for the pressure. **F** determines the load vector of the mixture (M) and of the fluid (F). Equation (3.4) shows the problem after the discretisation in the form of a matrix equation.

$$\begin{pmatrix} \mathbf{M}_{M1} & 0 & 0 \\ \mathbf{M}_{F1} & 0 & 0 \\ 0 & 0 & 0 \end{pmatrix} \begin{pmatrix} \mathbf{u}''_S \\ 0 \\ 0 \end{pmatrix} + \begin{pmatrix} \mathbf{D}_{M1} & \mathbf{D}_{M2} & 0 \\ \mathbf{D}_{F1} & \mathbf{D}_{F2} & 0 \\ \mathbf{D}_{K1} & 0 & 0 \end{pmatrix} \begin{pmatrix} \mathbf{u}'_S \\ \mathbf{w}'_F \\ 0 \end{pmatrix}$$
$$\begin{pmatrix} \mathbf{K}_{M1} & \mathbf{K}_{M2} & \mathbf{K}_{M3} \\ 0 & \mathbf{K}_{F2} & \mathbf{K}_{F3} \\ 0 & \mathbf{K}_{K2} & 0 \end{pmatrix} \begin{pmatrix} \mathbf{u}_S \\ \mathbf{w}_F \\ p \end{pmatrix} = \begin{pmatrix} \mathbf{F}^M \\ \mathbf{F}^F \\ 0 \end{pmatrix}. \tag{3.4}$$

The Newmark method was chosen for the time integration and with the help of the result of the last time step, the problem can be converted into a $n \times n$ matrix with an update of the load vector.

4. Examples

4.1. Consolidation problem

Taking the linear theory into account, DE BOER *et al.* [9] presented an analytical solution for an infinite halfspace using the Laplace transformation. Thus there is an excellent example for the comparison of the analytical and the numerical solution. In order to model the half-space via the finite element method, a column of 10 m depth and $2\,\mathrm{m}^2$ surface was taken into account. The solution was calculated for a very short time, so that no signal of the rigid boundary in 10 m depth could influence the solution. The upper boundary of the column is perfectly drained and loaded in the first case by a sine load (q):

$$q_1(t) = 3\sin(\omega\, t) \quad \left[\frac{\mathrm{kN}}{\mathrm{m}^2}\right], \qquad \omega = 75\ \mathrm{s}^{-1},$$

and in another case by a step load (q):

$$q_2(t) = 3 \quad \left[\frac{\mathrm{kN}}{\mathrm{m}^2}\right].$$

The other boundaries are undrained and rigid, see Fig. 1. The material parameters are taken from [9] as:

$$\begin{aligned} \mu^S &= 5583\ \mathrm{kN/m^2}, & \lambda^S &= 8375\ \mathrm{kN/m^2}, \\ \varrho^{SR} &= 2000\ \mathrm{kg/m^3}, & \varrho^{FR} &= 1000\ \mathrm{kg/m^3}, \\ n^S_{0S} &= 0.67, & k^f &= 0.01\ \mathrm{m/s}. \end{aligned}$$

As expected, the displacement-time behaviour starts with a large time-gradient, which decreases with passing time. We can compare this behaviour with a strong damped vibration-system, which has in fact the same structure after the dicretisation.

Figure 2 shows the surface displacement under both the loads. It shows a good agreement between the analytical and the numerical solution. In the case of the sine load, there is no visible difference between both the solutions.

In the example mentioned above, the external acceleration was neglected. Thus the calculation has started when the settlement under its own weight is finished. An interesting point is to show the settlement under its own weight, without an external load. This result is to be seen in Fig. 3.

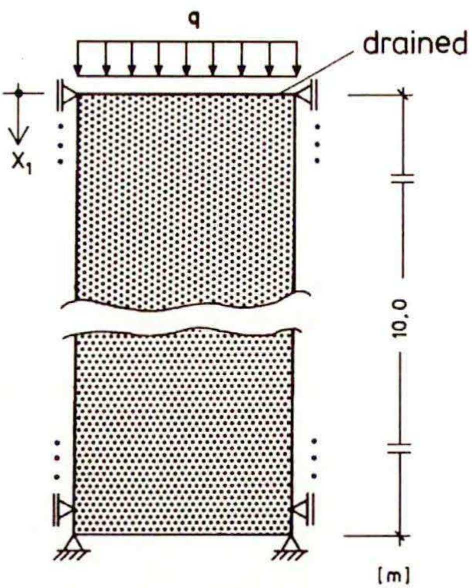

FIG. 1. Example.

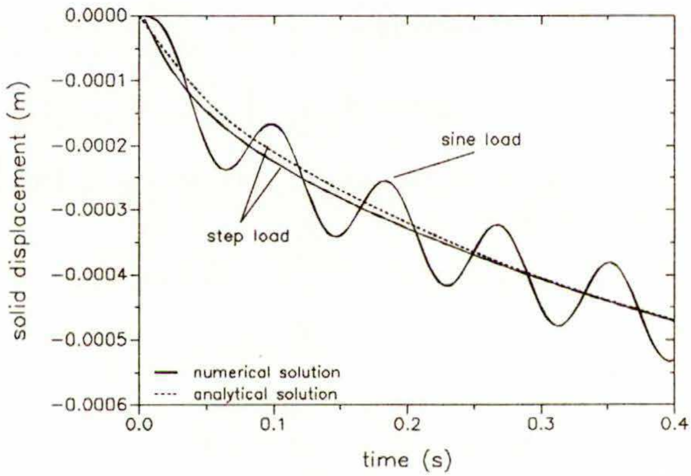

FIG. 2. Comparison between an analytical and a numerical solution.

We can see that at the begining, the weight of the whole column:

$$\int_V (\varrho^S + \varrho^F)\,\mathbf{b}\,dv = 167\,\mathrm{kN}\ [\mathbf{e}_1],$$

is causing the pore pressure. With the passage of time, the effective stress in the solid increases to $-\,67\,\mathrm{kN/m^2}$, and the pore pressure it decreases to $100\,\mathrm{kN/m^2}$,

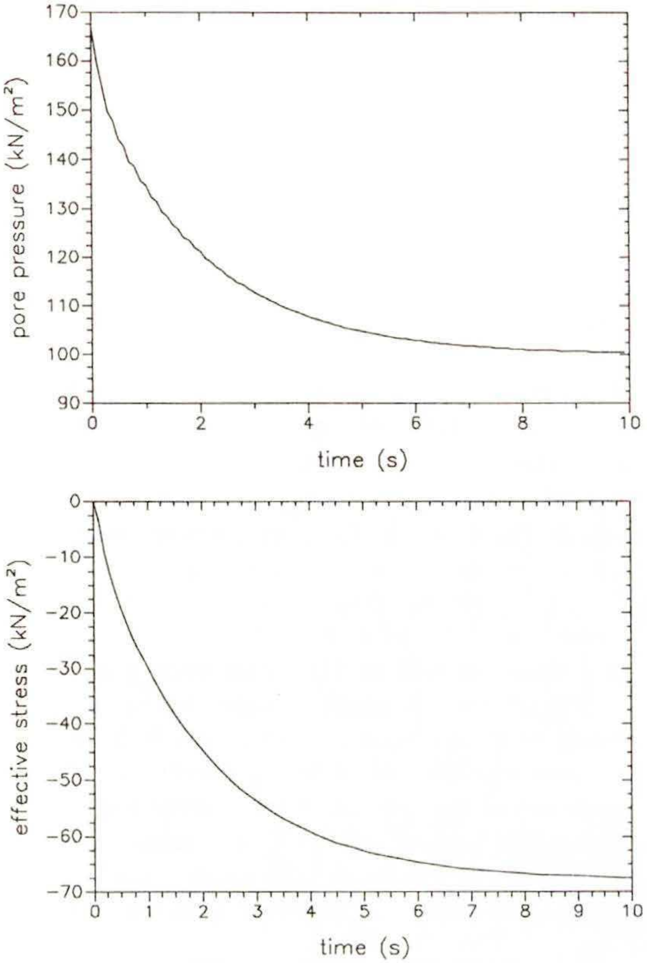

FIG. 3. Pore pressure and effective stress under its own weight.

which is the exact pore pressure of a water column of 10 m depth,

$$\int_0^{10} \varrho^{FR}\,\mathbf{b}\,dx = 100\,\mathrm{kN/m^2}.$$

The part of the weight entering the solid is exactly the weight of the solid minus the uplift:

$$\int_V n^S(\varrho^{SR} - \varrho^{FR})\,\mathbf{b}\,dv = 67\,\mathrm{kN}.$$

In the case of a linear theory we can neglect the external acceleration; only in the case, when we are intrested in the absolute value of the pore pressure, displacement or stress, we have to add the initial values.

4.2. One-dimensional wave propagation

The second example is the one-dimensional wave propagation in the same structure as shown in the first example, where only the Darcy parameter has changed: $k^f = 10\,\mathrm{m/s}$.

4.2.1. Step load. In the first case the column was once again loaded with the Heaviside function, but with a different amplitude: $q_3(t) = 100\,\mathrm{kN}$ (see Fig. 1).

According to BIOT'S theory [1], with two compressible constituents there are two longitudinal waves in a porous medium. One wave is transmitted through the fluid (P1-wave) and the other is transmitted through the elastic structure of the solid skeleton (P2-wave), see [11]. These two waves are coupled through the coupling effect produced by motions of the solid and fluid. In this article both constituents are incompressible, thus the speed of the wave transmitted through the fluid (P1-wave) is infinite.

This is illustrated by Fig. 4, where the pore pressure versus time is shown. The pore pressure at the bottom of the column changes directly from the static value of $100\,\mathrm{kN/m^2}$ up to the static value plus the external load per $\mathrm{m^2}$. This is according to the statement of TERZAGHI [13], where he found out that the whole external load is firstly carried by the water body and then, while water is flowing out, the solid skeleton is going to take the external load. In Fig. 4 there are some oscillations in the pressure, which result from the big jump in the pressure. Furthermore, the diagram shows when the disturbance is reflected from the bottom or the top of the column. If we observe Fig. 4 in detail, we can see that the pressure at the bottom is $100\,\mathrm{kN/m^2}$ (static value) + $100\,\mathrm{kN/m^2}$ (external load) = $200\,\mathrm{kN/m^2}$. In 2 m depth (this point in the Fig. 4 is called top), the value is $20\,\mathrm{kN/m^2}$ (static value) + $100\,\mathrm{kN/m^2}$ (external load) = $120\,\mathrm{kN/m^2}$.

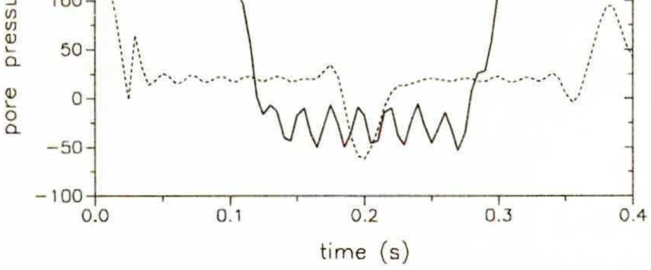

FIG. 4. Pore pressure versus time. — bottom, - - - top.

We see, that the information about the external load is transmitted with an infinite velocity through the incompressible fluid. The pore pressure at the top soon decreases to the static value of $20\,\mathrm{kN/m^2}$ as the solid skeleton takes up the external load. But it takes time till the disturbance travelling in the solid skeleton reaches the bottom of the column. This happens at $t = 0.1\,\mathrm{s}$, when the pore pressure decreases to the static value ($100\,\mathrm{kN/m^2}$).

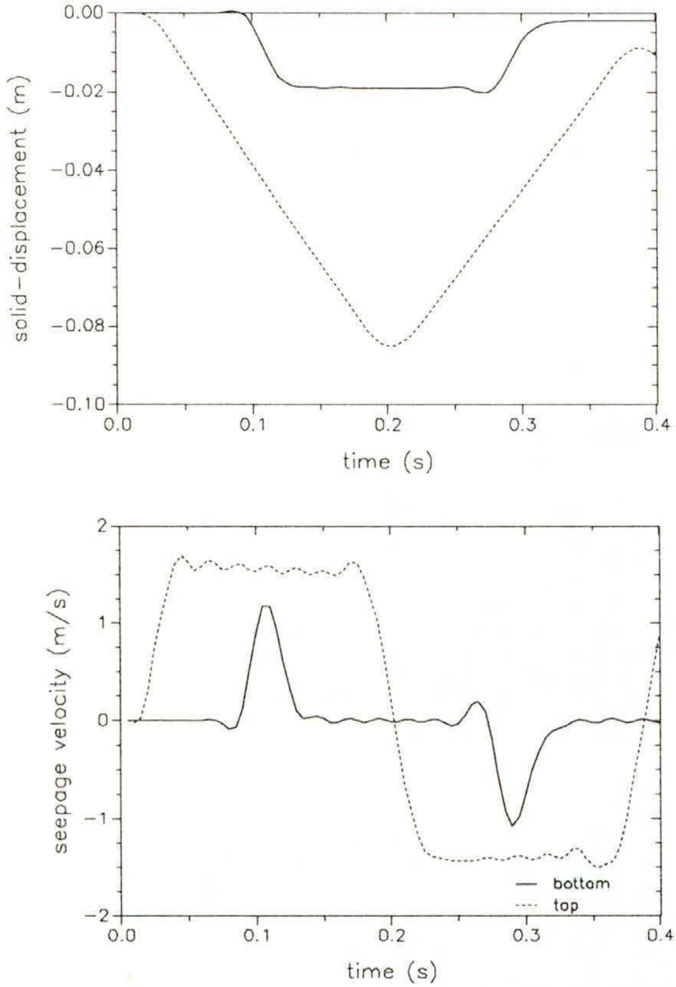

FIG. 5. Solid displacement and seepage velocity versus time.

In comparison with Fig. 5, where the solid displacement and the seepage velocity are shown, it can be observed that at time 0.1 s the P2-wave (transmitted by the elastic structure) hits the rigid bottom of the column and is reflected. This is coupled with a change in the pore pressure and the seepage velocity. At the time-instant 0.2 s, the P2-wave reaches the unfixed top of the column and the sign of the disturbance changes, see [6, 14]. At the time-instant 0.3 s the P2-wave hits the rigid bottom again, and at time 0.4 s one period of this procedure is closed.

4.2.2. Impulse load. Another good example to show the coupling between solid displacement and pore pressure is to load the column with an impulse load:

$$f_4(t) = \begin{cases} 100\sin(314.16/\mathrm{s}\,t)\,\mathrm{kN} & \text{for} \quad 0 < t < 0.01\,\mathrm{s}, \\ 0 & \text{for} \quad t > 0.01\,\mathrm{s}. \end{cases}$$

The dynamic response at time 0.02 s of the column, as described above, is shown in the Fig. 6, where the solid strain and the pore pressure are exhibited versus the length of the column. The top is at $x = 10$ m and the bottom at $x = 0$ m.

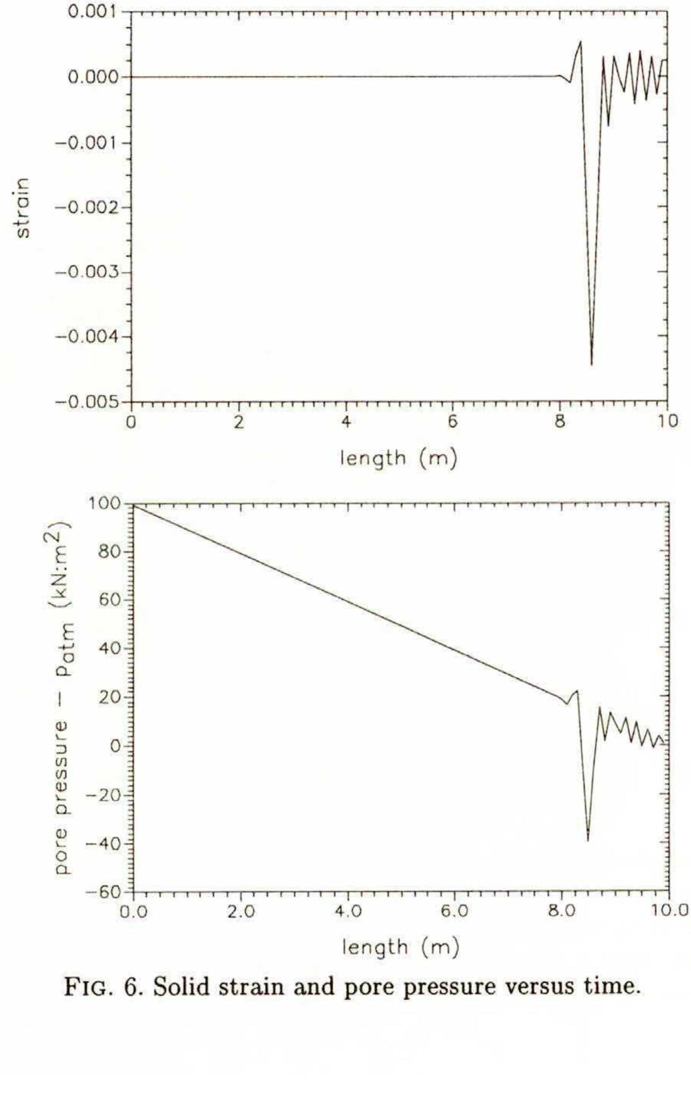

FIG. 6. Solid strain and pore pressure versus time.

The line in the pore pressure diagram from 100 to 0 [kN/m^2] is the static solution for the pore pressure under its own weight. We can see a disturbance travelling with the speed of the P2 wave in the pore pressure as well as in the solid strain.

5. Concluding remarks

The dynamic response of an incompressible fluid-saturated porous media is studied. The calculation via the finite element method is based upon the incompressible porous media model of DE BOER [8] and BLUHM [2]. The first application of this theory in this paper is the numerical solution of the consolidation problem. This numerical solution in comparison with the existing analytical solution shows a good agreement. In the second application the propagation of longitudinal waves is studied. According to Biot's theory (Biot treated compressible constituents), there are two longitudinal waves: a P1 wave transmitted by the pore fluid and a P2 wave transmitted by the elastic structure. This paper shows that the speed of the P1 wave, transmitted in the incompressible pore fluid, is infinite and only the P2 wave, transmitted by the elastic structure, can be observed in porous media with incompressible constituents.

Acknowledgments

The author is grateful to Prof. Dr.-Ing. R. DE BOER and Priv.-Doz. Dr.-Ing. J. BLUHM for their critical comments offered during the preparation of this paper. This work has been supported by the Deutsche Forschungsgemeinschaft (Germany).

References

1. M.A. BIOT, *Theory of propagation of elastic waves in fluid-saturated porous solid. 1. Lower-frequency range*, J. Acoust. Soc. Am., **28**, 168–178, 1956.
2. J. BLUHM, *A consistent model for saturated porous media*, Habilitation Thesis, University of Essen, 1996.
3. J. BLUHM and R. DE BOER, *The volume fraction concept in the porous media theory*, Report MECH 94/5, FB 10/Mechanik, Universität-GH Essen, to appear in: Zeitschrift für Angewandte Mathematik und Mechanik (ZAMM), 1994.
4. R.M. Bowen, *Incompressible porous media models by use of the theory of mixtures*, Int. J. Engng. Sci., **18**, 1129–1148, 1980.
5. R.M. Bowen, *Compressible porous media models by use of the theory of mixtures*, Int. J. Engng. Sci., **20**, 697–735, 1982.
6. S. BREUER, *Numerische Berechnung der Ausbreitung und Reflexion von longitudinal Wellen in linear elastischen Stäben*, pp. 51–66, [in:] Beiträge zur Mechanik, Festschrift zum 60. Geburtstag von Prof. Dr.-Ing. Reint de Boer, Forschungsbericht aus dem Fachbereich Bauwesen, **66**, Universität Essen, 1995.

7. R. DE BOER, *Vektor- und Tensorrechnung für Ingenieure*, Springer-Verlag, Berlin 1982.

8. R. DE BOER, *Highlights in the historical development of the porous media theory: Toward a consistent macroscopic theory*, Applied Mech. Reviews, **49**, 201–262, 1996.

9. R. DE BOER, W EHLERS and Z. LIU, *One-dimensional transient wave propagation in fluid-saturated incompressible porous media*, Arch. Appl. Mech., **63**, 59–72, 1993.

10. W. EHLERS, *Poröse Medien - ein kontinuumsmechanisches Modell auf der Basis der Mischungstheorie*, Forschungsbericht aus dem Fachbereich Bauwesen, **49**, 1989.

11. F.E. RICHART, J.R. HALL and R.D. WOODS, *Vibrations of soils and foundations*, Prentice-Hall, New Jersey 1970.

12. J.C. SIMO and K.S. PISTER, *Remarks on constitutive equations for the finite deformation problems: Computational implications*, Comp. Meth. Appl. Mech. Engng., **46**, 201–215, 1984.

13. K. VON TERZAGHI and R.B. PECK, *Soil mechanics in engineering practice*, Wiley, New York 1948.

14. F. ZIEGLER, *Technische Mechanik der festen und flüssigen Körper*, Springer Verlag, Wien 1985.

INSTITUTE OF MECHANICS, FB 10, UNIVERSITY OF ESSEN,
45117 ESSEN, GERMANY.

e-mail: breuer@mechanik.bauwesen.uni-essen.de

Received December 30, 1996; new version May 5, 1997.